


[¹⁸F]FP-(+)-DTBZ PET study in a lactacystin-treated rat model of Parkinson disease

Chi-Chang Weng¹ · Siao-Lan Huang² · Zi-An Chen² · Kun-Ju Lin^{3,4} ·
Ing-Tsung Hsiao^{2,3,4} · Tzu-Chen Yen³ · Mei-Ping Kung⁵ · Shiaw-Pyng Wey^{2,3,6}  ·
Ching-Han Hsu¹

Received: 28 February 2017 / Accepted: 24 April 2017 / Published online: 27 April 2017
© The Japanese Society of Nuclear Medicine 2017

Abstract

Objective Lactacystin has been used to establish rodent models of Parkinson disease (PD), with cerebral α -synuclein inclusions. This study evaluated the uptake of [¹⁸F]9-fluoropropyl-(+)-dihydrotrabenazine ([¹⁸F]FP-(+)-DTBZ), a vesicular monoamine transporter type 2 (VMAT2)-targeting radiotracer, through positron emission tomography (PET) in lactacystin-treated rat brains.

Methods Adult male Sprague–Dawley rats were randomly treated with a single intracranial dose of lactacystin (2 or 5 μ g) or saline (served as the sham control) into the left

medial forebrain bundle. A 30-min static [¹⁸F]FP-(+)-DTBZ brain PET scan was performed following an intravenous [¹⁸F]FP-(+)-DTBZ dose (approximately 22 MBq) in each animal at 2 and 3 weeks after lactacystin treatment. Upon completing the last PET scans, the animals were killed, and their brains were dissected for ex vivo autoradiography (ARG) and immunohistochemical (IHC) staining of tyrosine hydroxylase (TH) as well as VMAT2.

Results Both the 2- and 5- μ g lactacystin-treated groups exhibited significantly decreased specific [¹⁸F]FP-(+)-DTBZ uptake in the ipsilateral striata (I-ST) at 2 weeks (1.51 and 1.16, respectively) and 3 weeks (1.36 and 1.00, respectively) after lactacystin treatment, compared with the uptake in the corresponding contralateral striata (C-ST) (3.48 and 3.08 for the 2- and 5- μ g lactacystin-treated groups, respectively, at 2 weeks; 3.36 and 3.11 for the 2- and 5- μ g lactacystin-treated groups, respectively, at 3 weeks) and the sham controls (3.34–3.53). Lactacystin-induced decline in I-ST [¹⁸F]FP-(+)-DTBZ uptake was also demonstrated through ex vivo ARG, and the corresponding dopaminergic neuron damage was confirmed by the results of TH- and VMAT2-IHC studies.

Conclusions In this PD model, lactacystin-induced dopaminergic terminal damage in the ipsilateral striatum could be clearly visualized through in vivo [¹⁸F]FP-(+)-DTBZ PET imaging. This may serve as a useful approach for evaluating the effectiveness of new treatments for PD.

Electronic supplementary material The online version of this article (doi:10.1007/s12149-017-1174-3) contains supplementary material, which is available to authorized users.

Shiaw-Pyng Wey and Ching-Han Hsu contributed equally to this work.

✉ Shiaw-Pyng Wey
spwey@mail.cgu.edu.tw

✉ Ching-Han Hsu
cghsu@mx.nthu.edu.tw

¹ Department of Biomedical Engineering and Environmental Sciences, National Tsing Hua University, Hsinchu, Taiwan

² Department of Medical Imaging and Radiological Sciences, Chang Gung University, Taoyuan, Taiwan

³ Center for Advanced Molecular Imaging and Translation, Department of Nuclear Medicine, Chang Gung Memorial Hospital, Linkou, Taoyuan, Taiwan

⁴ Neuroscience Research Center, Chang Gung Memorial Hospital, Linkou, Taoyuan, Taiwan

⁵ Department of Radiology, University of Pennsylvania, Philadelphia, PA, USA

⁶ Institute of Radiological Research, Chang Gung University and Chang Gung Memorial Hospital, Taoyuan, Taiwan

Keywords Parkinson disease · Animal model · Lactacystin · PET imaging · Autoradiography

Introduction

Parkinson disease (PD) is the second most common neurodegenerative disease, following Alzheimer disease. The clinical symptoms of PD include resting tremors, postural instability, bradykinesia, and rigidity [1], and these clinical abnormalities result from the neurodegeneration of the dopamine system. Dopaminergic neurodegeneration has three common characteristics: (1) a huge loss of dopaminergic neurons (50–80%) in the substantia nigra (SN), (2) a profound decrease in the dopamine concentration of the striatum (ST), and (3) the pathophysiological presence of Lewy bodies (LBs) [2, 3]. However, the pathogenetic mechanism of PD remains unknown.

To explore the disease mechanism and evaluate the progression of PD, the combined use of *in vivo* positron emission tomography (PET) imaging and a PD-mimicking animal-model may provide an ideal solution. Many PET tracers aimed at the different binding pockets of presynaptic dopaminergic neurons have been developed in the last decade. For example, [¹¹C](+)-dihydrotrabenazine ([¹¹C](+)-DTBZ) has a suitable binding property ($K_i = 0.96$ nM) and specificity for vesicular monoamine transporter type 2 (VMAT2) [4–7]. However, the short physical half-life of ¹¹C (20 min) makes this tracer less desirable. To solve the availability problem of the VMAT2 tracer, [¹⁸F]9-fluoropropyl-(+)-dihydrotrabenazine ([¹⁸F]-FP-(+)-DTBZ), which has a relatively longer half-life (109 min), was developed [8, 9]; it also has a better binding affinity ($K_i = 0.1$ nM) than does [¹¹C](+)-DTBZ [10].

Currently, 6-hydroxydopamine (6-OHDA) and 1-methyl-4-phenyl-1,2,3,6-tetrahydropyridine (MPTP) are the two most commonly used neurotoxins for establishing animal models of PD. Both models exhibit nigrostriatal degeneration similar to that observed in idiopathic PD [11, 12] and can be successfully monitored for dopaminergic neuron loss *in vitro* and *in vivo*. However, both these models either do not show or have a limited expression of LBs, which are the most specific pathological hallmark of PD [13, 14].

LBs are mainly composed of α -synuclein inclusions and are located in the cytoplasm of affected dopaminergic

neurons [13, 14]. Abnormal α -synuclein accumulation within the affected neurons in the postmortem brain tissue of PD patients was related to ubiquitin proteasome system (UPS) dysfunction [15]. In accordance with the relevance of UPS dysfunction and expression of LBs, several studies have developed new animal models of PD through the administration of UPS inhibitors such as lactacystin [16–18]. Lactacystin injection methods are of two types: intracranial injection [19, 20] and systemic administration [21, 22]; however, the latter technique has shown some controversial results and is seldom used as a PD animal model [23–26].

The present study used *in vivo* PET imaging, as well as *ex vivo* autoradiography (ARG) with [¹⁸F]-FP-(+)-DTBZ to evaluate the dopaminergic neuron damage in rat brains after intracranial injection of lactacystin into the left medial forebrain bundle (L-MFB). In addition, the lactacystin-induced nigrostriatal lesion was assessed through immunohistochemical (IHC) staining.

Materials and methods

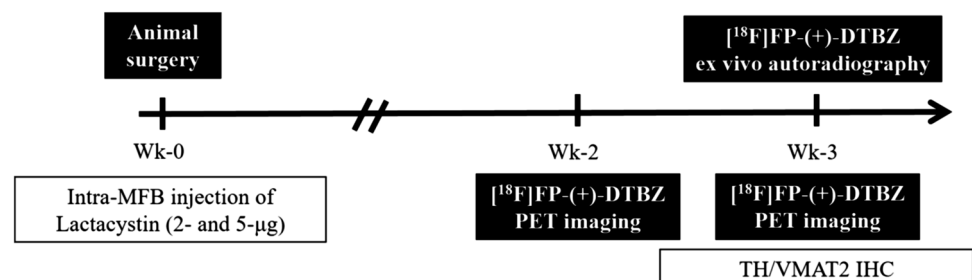
Experimental design

The experimental design used in this study is illustrated in Fig. 1. For the longitudinal investigation, all animals underwent [¹⁸F]-FP-(+)-DTBZ *in vivo* PET imaging to evaluate the dopaminergic neuron damage at 2 and 3 weeks after 2 or 5 μ g of lactacystin treatment. Following the last PET scan, *ex vivo* autoradiography (ARG) and IHC staining of tyrosine hydroxylase (TH) and VMAT2 were performed to confirm the lactacystin-induced dopaminergic neuron damage.

Animal preparation

Twelve Sprague–Dawley (SD) rats (male 300–350 g; Lasco, Yilan, Taiwan) were housed in clear cages in a controlled environment (temperature 22–25 °C) with a 12-h light/dark cycle, and were allowed to acclimate for a week with food and water available *ad libitum*. The animals were randomly assigned to different groups. A

Fig. 1 Experimental design



previously reported animal surgery protocol was followed [18]. Briefly, all animal surgery and injection procedures were performed under gas anesthesia (3% isoflurane in oxygen). After surgery, each rat received an intracranial injection containing either a different single dose of lactacystin (2 or 5 μg) or saline (vehicle of lactacystin, served as the sham control) into the left medial forebrain bundle (L-MFB) (AP -4.4 mm, ML -1.5 mm laterally from the bregma and 7.8 mm ventrally to the dura [27]). The procedures for the care of the rats and the experiments were approved by the Institutional Animal Care and Use Committee of Chang Gung University and followed the experimental animal care guidelines (IACUC approval number: CGU12-165).

Radiochemistry

Optically pure [^{18}F]FP-(+)-DTBZ was prepared at the cyclotron facility of Chang Gung Memorial Hospital (Taoyuan, Taiwan), using a precursor provided by Avid Radiopharmaceuticals, Inc. (Philadelphia, PA, USA). The radiochemical purity of [^{18}F]FP-(+)-DTBZ was greater than 98%, and the specific activity was 60–200 TBq/mmol at the end of synthesis [28].

In vivo PET scan and image analysis

All PET images were acquired using a preclinical Inveon PET system (Siemens Medical Solutions, Knoxville, TN, USA). The 2- and 5- μg lactacystin-treated animals were subjected to in vivo [^{18}F]FP-(+)-DTBZ PET scans at 2 and 3 weeks after lactacystin treatment, whereas the sham control rats were scanned at 3 weeks after surgery. A 30-min static brain PET scan was performed on each animal under isoflurane anesthesia at 1 h after receiving a single-bolus intravenous injection of [^{18}F]FP-(+)-DTBZ (approximately 22 MBq in 0.2 mL saline solution). Images were acquired with filter back projection mode, and then reconstructed using the 2D OSEM method with attenuation and scatter corrections using Co-57.

All imaging data were analyzed with PMOD software (version 3.2, PMOD Technologies, Zurich, Switzerland). Briefly, the individual PET image was manually fused with the built-in MR template, and then the VOIs of the ipsilateral striatum (I-ST), contralateral striatum (C-ST), and cerebellum (CB) from the MR template were applied for the PET image analysis (as shown in Fig. S1 in Online Resource). The striatal specific uptake ratio (SUR) was calculated as [(uptake in ST – uptake in CB)/(uptake in CB)], where the CB was applied as the reference region. The SUR ratio (I-ST to C-ST) of each animal was further calculated for analysis.

Ex vivo autoradiography

Immediately after the last [^{18}F]FP-(+)-DTBZ PET scan, ex vivo ARG was performed on the lactacystin-treated rats and sham controls. Briefly, the animals were euthanized through cervical dislocation, and their brains were quickly removed and frozen on dry ice. Next, coronal sections were cut on a cryostat microtome (CM3050S; Leica, Bensheim, Germany), with a thickness of 20 μm . After drying them out with a cool fan, the brain sections were exposed to a BAS SR2040 imaging plate (20 \times 40 cm^2 ; Fujifilm, Tokyo, Japan) overnight. The plate was scanned using a phosphor image reader (FLA-5100; Fujifilm, Tokyo, Japan).

Immunohistochemistry

To confirm the lactacystin-induced selective damage of dopaminergic neurons, the striatal and the substantial nigra (SN) sections were prepared for IHC staining with rabbit anti-TH and rabbit anti-VMAT2 antibodies. DAB (3,3'-diaminobenzidine) staining was performed by employing an UltraVision Quanto Detection System HRP DAB kit (Thermo Scientific, CA, USA). The conditions for the primary antibodies of TH (AB152; Millipore, Temecula, CA, USA) and VMAT2 (ab81855; Abcam, Cambridge, UK) were 1:500 and 1:2000, respectively, and the antibodies were incubated for 30 min. Upon completing the staining, the slides were photographed under an optical microscope (Eclipse E600; Nikon, Tokyo, Japan) equipped with a digital camera (DS-Fi1; Nikon, Tokyo, Japan).

Statistical analysis

All data are presented as mean \pm standard deviation (SD). Differences between the groups were assessed through a one-way ANOVA, followed by the Student–Newman–Keuls post hoc test. Values of $P < 0.05$ were considered statistically significant.

Results

In vivo PET imaging and image analysis

Prior to initiating the PET study, the optimal imaging time window to reach the plateau ST-to-CB ratio was determined to be 1 h from the time-activity curve (as shown in Fig. S2 in Online Resource) after the intravenous injection of [^{18}F]FP-(+)-DTBZ in three normal SD rats.

Figure 2 shows the representative PET images of the different animal groups at 2 and 3 weeks after lactacystin treatment. Data obtained from the sham control group

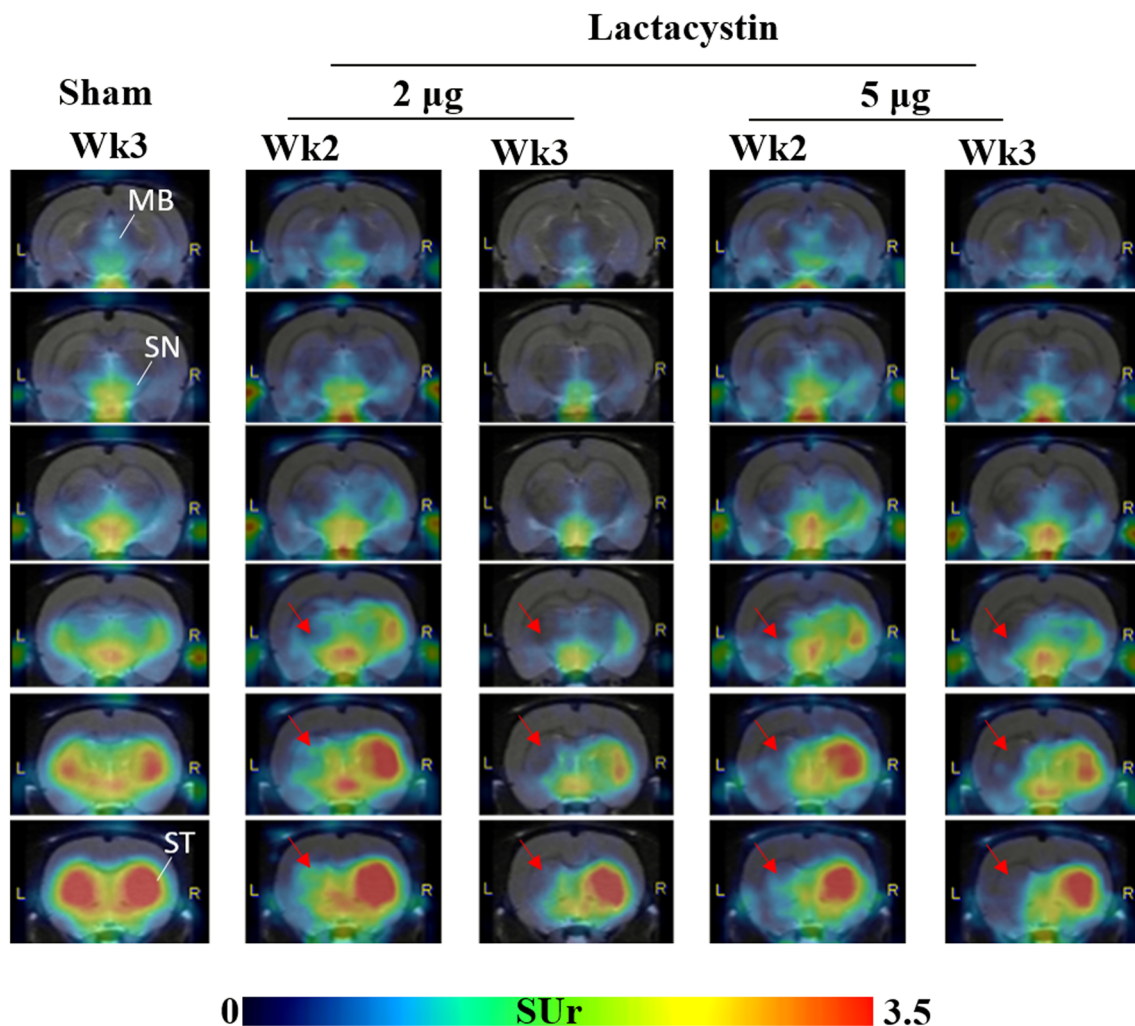


Fig. 2 Representative [^{18}F]FP-(+)-DTBZ PET images of the brains of the rat groups at 2 and 3 weeks after lactacystin treatment and at 3 weeks after surgery in the sham control group. All PET images

were coregistered to a PMOD built-in T2 MR template and were scaled according to the SUr level. *ST* striatum, *SN* substantia nigra, *MB* midbrain; *red arrows* indicate the lesion sides

revealed no obvious differences between the I-ST and C-ST uptakes, indicating that no obvious physical damage was caused by the intracranial surgery procedure. By contrast, in all lactacystin-treated animal groups (regardless of dose and time point differences), substantially less uptake was noted on the injected side. A comparison of the I-ST uptake between the 2- and 5- μg groups at 2 weeks after lactacystin injection revealed that the 5- μg group showed a greater decline in uptake than did the 2- μg group. However, at 3 weeks after treatment, the decreases in uptake were almost the same between the groups, which might indicate a plateau in the damage caused by lactacystin in the late phase.

Quantified data from the [^{18}F]FP-(+)-DTBZ PET images for different lactacystin doses and time points are summarized in Table 1. The decline in SUr values of the I-ST at 2 and 3 weeks after lactacystin treatment was 57

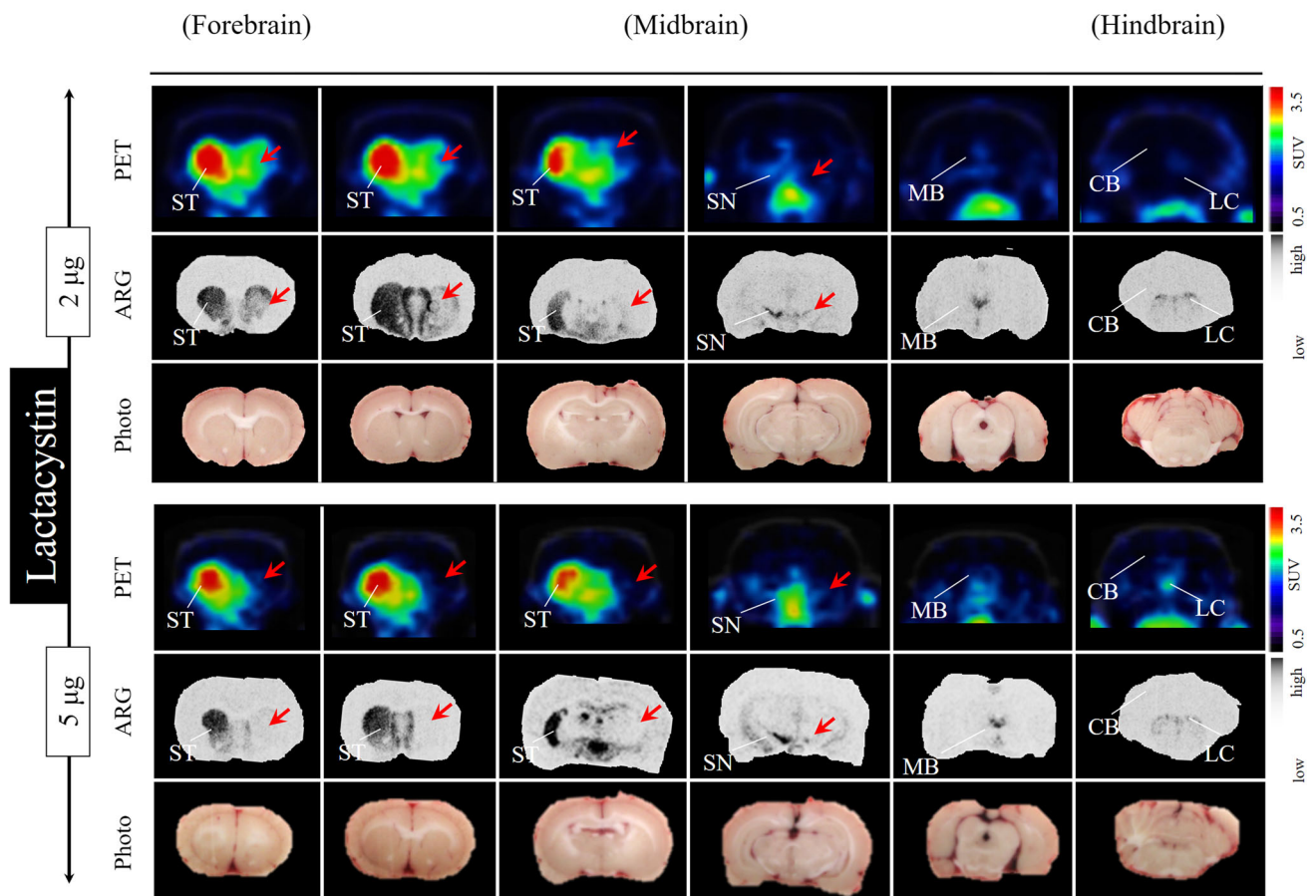
and 60% for the 2- μg animal group and 62 and 68% for the 5- μg animal group, respectively.

Ex vivo autoradiography

The ARG images for the 2- and 5- μg lactacystin-injected animal groups obtained at 3 weeks after treatment are shown in Fig. 3; the corresponding PET and photographic images are parallelly presented for comparison. The ARG results indicated an obvious decrease in [^{18}F]FP-(+)-DTBZ uptake in the I-ST of both the animal groups, a finding which aligned with the PET imaging results. Moreover, small dopaminergic neuron-rich areas (such as the SN), which are difficult to visualize through PET, could be easily assessed through ARG. Therefore, ARG could be a critical supplement for animal PET to investigate the signal changes in regions with a small volume.

Table 1 Quantitative striatal uptake of [¹⁸F]FP-(+)-DTBZ in rat brains after lactacystin treatment

Animal group	Brain region	[¹⁸ F]FP-(+)-DTBZ SUR ^a		SUR ratio (I-ST to C-ST)	
		2 weeks	3 weeks	2 weeks (%)	3 weeks (%)
Sham	I-ST	3.34 ± 0.17	3.42 ± 0.26	95	100
	C-ST	3.53 ± 0.29	3.43 ± 0.22		
2-μg	I-ST	1.51 ± 0.52	1.36 ± 0.32	43	40
	C-ST	3.48 ± 0.35	3.36 ± 0.35		
5-μg	I-ST	1.16 ± 0.21*	1.00 ± 0.28*	38	32
	C-ST	3.08 ± 0.44	3.11 ± 0.63		

* $P < 0.05$, compared with corresponding contralateral side^a SUR data are presented as mean ± SD ($n = 4$ for each group)**Fig. 3** Representative ex vivo ARG images of rat brain sections presented parallelly with the corresponding PET and photographic images of the different animal groups at 3 weeks after lactacystintreatment. *ST* striatum, *SN* substantia nigra, *MB* midbrain, *CB* cerebellum, *LC* locus coeruleus; *red arrows* indicate the lesion sides

Immunohistochemistry

The brain sections with lactacystin-induced decline in [¹⁸F]FP-(+)-DTBZ uptake observed on the PET and ARG images were further evaluated for dopaminergic neuron damage, through TH and VMAT2 IHC staining. Representative TH and VMAT2 IHC staining images of the I-ST and TH IHC staining images of the SN in the different

animal groups are shown in Fig. 4a, b, respectively. A decline in TH and VMAT2 expression in the I-ST and a decrease in TH expression in the SN were observed in the lactacystin-treated groups. The images of TH and VMAT2 IHC staining of the I-ST in each animal group (Fig. 4a) were further digitized, and the values were quantified as percentage ratios to the corresponding C-ST values (Fig. 4c). Decreases in TH expression in the I-ST of

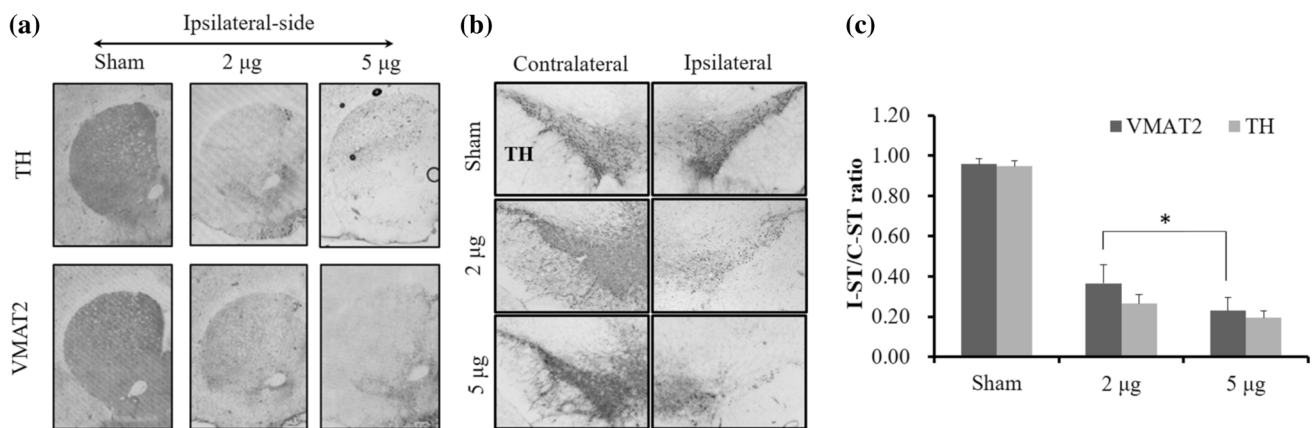


Fig. 4 IHC results for the ST and SN regions of the different animal groups. **a** The representative TH and VMAT2 IHC staining images of the I-ST. **b** TH IHC staining images of the SN. **c** Quantification of the TH and VMAT2 IHC staining data for the I-ST and the corresponding

C-ST. * $P < 0.05$. *ST* striatum, *SN* substantia nigra, *I-ST* ipsilateral striatum, *C-ST* contralateral striatum, *VMAT2* type two vesicular monoamine transporter, *TH* tyrosine hydroxylase

approximately 70 and 80% were noted in the 2- and 5- μ g lactacystin-treated animal groups, respectively.

Discussion

In vivo imaging techniques such as PET have many excellent abilities, including the monitoring of disease progression and screening for therapeutic response. Recently, with the increasing requirement of PET imaging for diagnosing PD patients, many novel tracers have been developed. [^{18}F]FP-(+)-DTBZ used in the present study has been well validated for its highly specific binding ability for VMAT2 and internal radiation dosimetry in humans [28], and can provide early, progressive, and severity information of dopaminergic neuron degeneration for the diagnosis of Parkinson disease [29, 30]. To explore the possible pathogenetic factors and develop new treatment strategies for PD, appropriate animal models of this neurodegenerative disease are always important for evaluation. Despite great success with huge dopaminergic neuron loss, some reverse treatment responses were noted in commonly used 6-OHDA- and MPTP-induced PD animal models [11, 12]; these findings could not be directly applied to humans [31], implying that PD pathogenesis in humans may differ from that in the most commonly used PD animal models.

In the last decade, UPS dysfunction has been confirmed through postmortems of PD patients and has been linked to α -synuclein, the core component of LBs, which are the pathological hallmark of PD [15]. Despite many efforts to develop α -synuclein-expressing PD models using UPS inhibitors such as lactacystin [16–26], many uncertainties, such as the dose of the UPS inhibitors and time after injection, remain unresolved.

In this study, longitudinal in vivo [^{18}F]FP-(+)-DTBZ PET imaging was performed in rats at 2 and 3 weeks after receiving a single intracranial dose of 2 or 5 μ g lactacystin into the L-MFB region. Two different lactacystin doses were used to induce medium and severe lesion levels of dopamine neuron degeneration. PET imaging revealed a severe decrease in [^{18}F]FP-(+)-DTBZ uptake in the I-ST of both animal groups and at two different time points, whereas the [^{18}F]FP-(+)-DTBZ uptake in the C-ST did not significantly differ from that in the sham control group. The results of the PET study implied that the lactacystin treatment performed in the present study could efficiently induce dopaminergic neuron damage within 2 weeks; this was consistent with previous findings [32]. The quantified PET image data, which were obtained through normalization of the I-ST values to the corresponding C-ST values in each animal, indicated an approximately 60–70% decline in [^{18}F]FP-(+)-DTBZ uptake. This finding was comparable with the results of a [^{11}C](+)-DTBZ PET study reported by Mackey et al. [33].

Due to the limited resolution of current small-animal PET imaging techniques, evaluating the dopaminergic neuron damage in every cerebral subregion of lactacystin-treated animals is challenging. To overcome this issue in the present study, ex vivo ARG was performed immediately after the PET scan. On comparing the ARG and PET images, the contour was clearly delineated in the ARG images and was superior to that of the PET images. Additionally, the [^{18}F]FP-(+)-DTBZ uptake in the lesion (injected) side of the SN was significantly decreased in lactacystin-treated rat brains. This finding revealed that the intracranial administration of lactacystin into the MFB not only caused dopaminergic terminal damage but also induced dopaminergic neuron degeneration. These results coincide with the findings of other studies using intranigral lactacystin injections [16–18, 32].

To further evaluate the status of lactacystin-induced dopaminergic neuron damage, the TH and VMAT2 expressions in the ST and SN were evaluated through IHC staining. The significant decreases in TH and VMAT2 expression on the injected sides of the ST and SN regions of the rat brains treated with either 2 or 5 µg of lactacystin aligned with the results of ex vivo ARG and in vivo PET imaging.

Conclusions

Dopaminergic neuron damage in rat brains treated with different intracranial doses of lactacystin at various time points was successfully evaluated using [¹⁸F]FP-(+)-DTBZ PET imaging. The results of PET imaging were verified using ex vivo ARG, as well as TH and VMAT2 IHC studies. Our findings indicate that [¹⁸F]FP-(+)-DTBZ PET imaging can be potentially valuable for investigating longitudinal dopaminergic neuron damage in a lactacystin-treated rat model of PD.

Acknowledgements This study was supported by grants from the Ministry of Science and Technology in Taiwan (NSC 100-2314-B-182A-092-MY3, NSC 102-2221-E-007-021-MY2, NSC 102-2314-B-182-049-MY3, and NSC 103-2623-E-182-001-NU) and the Research Fund of Chang Gung Memorial Hospital (CMRPG3A0513 and CMRPG391514). We thank Eli Lilly/Avid Radiopharmaceuticals (Philadelphia, PA, USA) for providing the precursor for the preparation of ¹⁸F-FP-(+)-DTBZ. The authors are also grateful to the Center for Advanced Molecular Imaging and Translation in the Department of Nuclear Medicine at Chang Gung Memorial Hospital in Linkou, Taoyuan, Taiwan. No potential conflicts of interest were disclosed.

References

- Massano J, Bhatia KP. Clinical approach to Parkinson's disease: features, diagnosis, and principles of management. *Cold Spring Harb Perspect Med*. 2012;2:a008870.
- Miller WC, DeLong MR. Parkinsonian symptomatology. An anatomical and physiological analysis. *Ann N Y Acad Sci*. 1988;515:287–302.
- Braak H, Braak E, Yilmazer D, Schultz C, de Vos RA, Jansen EN. Nigral and extranigral pathology in Parkinson's disease. *J Neural Transm Suppl*. 1995;46:15–31.
- Moore DJ, West AB, Dawson VL, Dawson TM. Molecular pathophysiology of Parkinson's disease. *Annu Rev Neurosci*. 2005;28:57–87.
- Bohnen NI, Albin RL, Koeppe RA, Wernette KA, Kilbourn MR, Minoshima S, et al. Positron emission tomography of monoaminergic vesicular binding in aging and Parkinson disease. *J Cereb Blood Flow Metab*. 2006;26:1198–212.
- Frey KA, Koeppe RA, Kilbourn MR. Imaging the vesicular monoamine transporter. *Adv Neurol*. 2001;86:237–47.
- Kilbourn MR, Frey KA, Vander Borcht T, Sherman PS. Effects of dopaminergic drug treatments on in vivo radioligand binding to brain vesicular monoamine transporters. *Nucl Med Biol*. 1996;23:467–71.
- Goswami R, Ponde DE, Kung MP, Hou C, Kilbourn MR, Kung HF. Fluoroalkyl derivatives of dihydrotrabenazine as positron emission tomography imaging agents targeting vesicular monoamine transporters. *Nucl Med Biol*. 2006;33:685–94.
- Kung MP, Hou C, Lieberman BP, Oya S, Ponde DE, Blankmeyer E, et al. In vivo imaging of β-cell mass in rats using ¹⁸F-FP-(+)-DTBZ: a potential PET ligand for studying diabetes mellitus. *J Nucl Med*. 2008;49:1171–6.
- Kung MP, Hou C, Goswami R, Ponde DE, Kilbourn MR, Kung HF. Characterization of optically resolved 9-fluoropropyl-dihydrotrabenazine as a potential PET imaging agent targeting vesicular monoamine transporters. *Nucl Med Biol*. 2007;34:239–46.
- Ungerstedt U. 6-Hydroxy-dopamine induced degeneration of central monoamine neurons. *Eur J Pharmacol*. 1968;5:107–10.
- Langston JW, Ballard PA Jr. Parkinson's disease in a chemist working with 1-methyl-4-phenyl-1,2,5,6-tetrahydropyridine. *N Engl J Med*. 1983;309:310.
- Shimoji M, Zhang L, Mandir AS, Dawson VL, Dawson TM. Absence of inclusion body formation in the MPTP mouse model of Parkinson's disease. *Brain Res Mol Brain Res*. 2005;134:103–8.
- Duty S, Jenner P. Animal models of Parkinson's disease: a source of novel treatments and clues to the cause of the disease. *Br J Pharmacol*. 2011;164:1357–91.
- Spillantini MG, Crowther RA, Jakes R, Hasegawa M, Goedert M. Alpha-synuclein in filamentous inclusions of Lewy bodies from Parkinson's disease and dementia with Lewy bodies. *Proc Natl Acad Sci USA*. 1998;95:6469–73.
- McNaught KS, Belizaire R, Jenner P, Olanow CW, Isacson O. Selective loss of 20S proteasome alpha-subunits in the substantia nigra pars compacta in Parkinson's disease. *Neurosci Lett*. 2002;326:155–8.
- Vernon AC, Johansson SM, MODO MM. Non-invasive evaluation of nigrostriatal neuropathology in a proteasome inhibitor rodent model of Parkinson's disease. *BMC Neurosci*. 2010;11:1.
- Vernon AC, Crum WR, Johansson SM, MODO M. Evolution of extra-nigral damage predicts behavioural deficits in a rat proteasome inhibitor model of Parkinson's disease. *PLoS One*. 2011;6:e17269.
- Fornai F, Lenzi P, Gesi M, Ferrucci M, Lazzeri G, Busceti CL, et al. Fine structure and biochemical mechanisms underlying nigrostriatal inclusions and cell death after proteasome inhibition. *J Neurosci*. 2003;23:8955–66.
- Miwa H, Kubo T, Suzuki A, Nishi K, Kondo T. Retrograde dopaminergic neuron degeneration following intrastriatal proteasome inhibition. *Neurosci Lett*. 2005;380:93–8.
- McNaught KS, Perl DP, Brownell AL, Olanow CW. Systemic exposure to proteasome inhibitors causes a progressive model of Parkinson's disease. *Ann Neurol*. 2004;56:149–62.
- McNaught KS, Olanow CW. Proteasome inhibitor-induced model of Parkinson's disease. *Ann Neurol*. 2006;60:243–7.
- Bové J, Zhou C, Jackson-Lewis V, Taylor J, Chu Y, Rideout HJ, et al. Proteasome inhibition and Parkinson's disease modeling. *Ann Neurol*. 2006;60:260–4.
- Manning-Boğ AB, Reaney SH, Chou VP, Johnston LC, McCormack AL, Johnston J, et al. Lack of nigrostriatal pathology in a rat model of proteasome inhibition. *Ann Neurol*. 2006;60:256–60.
- Kordower JH, Kanaan NM, Chu Y, Suresh Babu R, Stansell J, Terpstra BT, et al. Failure of proteasome inhibitor administration to provide a model of Parkinson's disease in rats and monkeys. *Ann Neurol*. 2006;60:264–8.
- Mathur BN, Neely MD, Dyllick-Brenzinger M, Tandon A, Deutch AY. Systemic administration of a proteasome inhibitor does not cause nigrostriatal dopamine degeneration. *Brain Res*. 2007;1168:83–9.

27. Paxinos G. The rat brain in stereotaxic coordinates—the new coronal set. 5th ed. Cambridge: Elsevier Academic Press; 2004.
28. Lin KJ, Weng YH, Wey SP, Hsiao T, Lu CS, Skovronsky D, et al. Whole-body biodistribution and radiation dosimetry of ^{18}F -FP-(+)-DTBZ (^{18}F -AV-133): a novel vesicular monoamine transporter 2 imaging agent. *J Nucl Med*. 2010;51:1480–5.
29. Okamura N, Villemagne VL, Drago J, Pejoska S, Dhamija RK, Mulligan RS, Ellis JR, Ackermann U, O’Keefe G, Jones G, Kung HF. In vivo measurement of vesicular monoamine transporter type 2 density in Parkinson disease with ^{18}F -AV-133. *J Nucl Med*. 2010;51(2):223–8.
30. Hsiao T, Weng YH, Hsieh CJ, Lin WY, Wey SP, Kung MP, Yen TC, Lu CS, Lin KJ. Correlation of Parkinson disease severity and ^{18}F -DTBZ positron emission tomography. *JAMA neurology*. 2014;71(6):758–66.
31. Bonsi P, Cuomo D, Martella G, Sciamanna G, Tolu M, Calabresi P, et al. Mitochondrial toxins in Basal Ganglia disorders: from animal models to therapeutic strategies. *Curr Neuropharmacol*. 2006;4:69–75.
32. Lorenc-Koci E, Lenda T, Antkiewicz-Michaluk L, Wardas J, Domin H, Śmiałowska M, et al. Different effects of intranigral and intrastriatal administration of the proteasome inhibitor lactacystin on typical neurochemical and histological markers of Parkinson’s disease in rats. *Neurochem Int*. 2011;58:839–49.
33. Mackey S, Jing Y, Flores J, Dinelle K, Doudet DJ. Direct intranigral administration of an ubiquitin proteasome system inhibitor in rat: behavior, positron emission tomography, immunohistochemistry. *Exp Neurol*. 2013;247:19–24.